

# Direct Solvation of Glycoproteins by Salts in Spider Silk Glues Enhances Adhesion and Helps To Explain the Evolution of Modern Spider Orb Webs

Vasav Sahni,<sup>†</sup> Toshikazu Miyoshi,<sup>†</sup> Kelley Chen,<sup>†</sup> Dharamdeep Jain,<sup>†</sup> Sean J. Blamires,<sup>‡</sup> Todd A. Blackledge,<sup>§</sup> and Ali Dhinojwala<sup>\*,†</sup>

<sup>†</sup>Department of Polymer Science, The University of Akron, Akron, Ohio 44325-3909, United States

<sup>‡</sup>Department of Life Sciences, Tunghai University, Taichung 40704, Taiwan

<sup>§</sup>Department of Biology, Integrated Bioscience Program, The University of Akron, Akron, Ohio 44325-3908, United States

## S Supporting Information

**ABSTRACT:** The evolutionary origin of modern viscid silk orb webs from ancient cribellate silk ancestors is associated with a 95% increase in diversity of orb-weaving spiders, and their dominance as predators of flying insects, yet the transition's mechanistic basis is an evolutionary puzzle. Ancient cribellate silk is a dry adhesive that functions through van der Waals interactions. Viscid threads adhere more effectively than cribellate threads because of the high extensibility of their axial silk fibers, recruitment of multiple glue droplets, and firm adhesion of the viscid glue droplets. Viscid silk's extensibility is permitted by the glue's high water content, so that organic and inorganic salts present in viscid glue droplets play an essential role in contributing to adhesion by sequestering the atmospheric water that plasticizes the axial silk fibers. Here, we provide direct molecular and macro-scale evidence to show that salts also cause adhesion by directly solvating the glycoproteins, regardless of water content, thus imparting viscoelasticity and allowing the glue droplets to establish good contact. This "dual role" of salts, plasticizing the axial silk indirectly through water sequestration and directly solvating the glycoproteins, provides a crucial link to the evolutionary transition from cribellate silk to viscid silk. In addition, salts also provide a simple mechanism for adhering even at the extremes of relative humidity, a feat eluding most synthetic adhesives.



## INTRODUCTION

Adhesives are used by biological organisms for locomotion, prey capture, and defense. The nature of adhesives ranges from the use of specialized chemistry such as DOPA-rich (dihydroxyphenylalanine-rich) adhesive plaques in marine mussels<sup>1</sup> to completely dry adhesives<sup>2</sup> based on van der Waals interactions<sup>3</sup> in geckos. There are also elegant examples of capillary forces used by tree frogs<sup>4</sup> and fast-curing cementlike underwater glues used by barnacles.<sup>5</sup> These various biological adhesives present a fertile ground of ideas for synthesizing synthetic adhesives that perform like, or better than, those used in nature. Perhaps one of the oldest and most interesting of these is the adhesive used by orb-weaving spiders. Spiders combine clever behavioral strategies with nearly invisible, high-performance, adhesive capture silk threads spun into a diverse array of prey-capture webs.<sup>6</sup> Orb-weaving spiders became dominant predators of flying insects after evolving a novel viscid capture thread, which replaced ancient dry cribellate capture thread, at least 150 million years ago.<sup>6</sup> A single evolutionary origin of viscid orb weavers from cribellate ancestors is well-established,<sup>6</sup> yet this transition is difficult to understand because viscid silk must be wet while cribellate silk must be dry to maintain adhesion.

Viscid threads are intricate composites of viscoelastic axial silk fibers covered by micrometer-sized glue droplets<sup>7</sup> that contain adhesive glycoproteins<sup>8</sup> surrounded by an aqueous solution consisting of low-molecular weight organic and inorganic compounds (collectively termed "salts").<sup>9</sup> Glycoproteins and salts are present in an aqueous dope in the aggregate silk glands of modern araneoid orb-weaving spiders.<sup>10</sup> Spiders coat flagelliform silk fibers with this dope when spinning the capture spirals of their orb webs. Rayleigh instability causes the initially homogeneous glue coating to self-organize into an array of micrometer-sized droplets.<sup>11</sup> These droplets then develop a phase-separated morphology consisting of a dense glycoprotein core surrounded by a sparse and translucent shell.<sup>11</sup> Recently, the shell was hypothesized to include a second layer of glycoproteins that is in turn surrounded by a fluid covering consisting of the aqueous salt solution.<sup>12</sup>

Studies based on *Nephila*, *Araneus*, and *Argiope* viscid threads show that the viscoelastic axial silk fibers are spun from the flagelliform glands and that the GPGGX amino acid motif

Received: December 8, 2013

Revised: January 26, 2014

Published: March 3, 2014

(where X can be Ala, Ser, Tyr, and Val)<sup>13,14</sup> appears as ~63 tandem repeats in the protein.<sup>15</sup> This repeat conforms to a  $\beta$ -spiral and thus facilitates the elastomeric behavior of viscid silk.<sup>16</sup> The surrounding glycoprotein glue is composed of two unique protein subunits, ASG1 and ASG2 (65 and 38 kDa, respectively). Both ASG1 and ASG2 are O-glycosylated. ASG1 has a high proportion of charged amino acids and is highly similar to chitin-binding proteins, while ASG2 has similarities with elastin and flagelliform silk protein and is thus associated with elasticity.<sup>17</sup> The carbohydrates associated with the adhesive glycoproteins are N-acetylgalactosamine, mannose, galactose, and fucose.<sup>18</sup>

Viscid capture threads, unlike cribellate threads, maximize their stickiness by summing the adhesive forces of multiple glue droplets as they extend in a suspension bridge-like mechanism so that crack propagation is resisted at multiple points along the thread.<sup>12</sup> This suspension bridge mechanism is possible in viscid threads because of the high extensibility of the axial silk and the firm adhesion of viscid glue droplets. The atmospheric water sequestered by the salts plasticizes the axial silk, thus producing its extreme extensibility,<sup>19</sup> a mechanism missing in cribellate axial threads.<sup>20</sup> These salts are present in large amounts<sup>9</sup> and are physiologically and nutritionally essential for the spiders,<sup>21</sup> suggesting that the salts may play a more prominent role in promoting adhesion than simply attracting water. Here, we provide direct molecular and macro-scale experimental evidence and develop a theoretical model to test the hypothesis that the salts directly generate adhesion by solvating and softening the glycoproteins themselves, even when dry, thereby facilitating adhesion in viscid threads via a “dual mechanism”. To support our hypothesis, we test two specific predictions. (1) Glycoproteins interact intimately with water, and are solvated by water, only in the presence of salts. (2) Salts are necessary for the glycoproteins to demonstrate humidity-dependent mobility, such that even at high levels of humidity, glycoproteins are highly mobile only in the presence of the salts.

This critical role of salts in adhesion of viscid threads sheds light on how the evolutionary transition from ancient webs utilizing dry cribellate nanofibers (primitive cribellar threads) to modern viscid glue orb webs could have occurred through an intermediate stage of dry but salty adhesive (derived cribellar threads).

## ■ EXPERIMENTAL SECTION

**Nuclear Magnetic Resonance (NMR) Experiments.** *NMR Sample Preparation.* To study the molecular-level interactions of water with salts, structural silk proteins, and adhesive glycoproteins (the main constituents of modern orb webs), solid-state nuclear magnetic resonance (SS-NMR) was used for the first time on viscid threads. We used four different solid-state NMR techniques to investigate the critical role of salt in enhancing adhesion by comparing spectra of webs with and without salts. A total of 74 female adult *Larinioides cornutus* spiders were fed with a 3% aqueous solution of 99% <sup>13</sup>C-labeled D-glucose (Sigma Aldrich) for 10 days before they were allowed to spin webs. Then 70 whole orb webs were collected on a clean glass capillary and subjected to a series of NMR analyses after exposure to different humidity values [dry, ambient, and 100% relative humidity (RH)]. The salts were then removed from the sample and the NMR analyses repeated under each condition.

To initially desiccate the sample, the glass capillary with webs wound on it was exposed to P<sub>2</sub>O<sub>5</sub> for ~48 h (0% RH). For room humidity testing, the same glass capillary was kept in a dust-free open container for 48 h, in a humidity-controlled room (50% RH). For the high-humidity testing, the same glass capillary was exposed to a sealed

90% humidity container for 48 h. Then, to remove the salts contained in the glue, the same glass capillary, with the webs wound over it, was immersed in deionized water and sonicated at 42 kHz in a Branson 1510 for ~1 h. The temperature of water increased from 26 to 43 °C after sonication for 1 h, which did not result in any permanent changes in the adhesion or tensile properties of the viscid silk. The washed web samples were then dried over P<sub>2</sub>O<sub>5</sub> and exposed to the desired level of humidity at room temperature as explained above for the pristine web sample. After exposure to the desired level of humidity, the glass capillary was immediately packed homogeneously into the NMR tube and sealed using Teflon tape. The changes in humidity during the experiments were minimal as confirmed by collecting the NMR spectra as a function of temperature over a period of 7 h (Figure S1 of the Supporting Information). The chamber used for desiccation was maintained at ~0% RH at 25 °C. The room humidity was maintained at ~50% RH, while the high-humidity chambers were maintained around ~90% RH at 25 °C.

To identify the salts in the glue and to verify that washing did not remove proteins, 0.1 mL of the aqueous extract from the wash was mixed with 0.6 mL of 99.96% D<sub>2</sub>O to perform solution-state <sup>1</sup>H NMR measurements (Figure S2 of the Supporting Information). Also, to check if sonication itself altered the silk, viscid threads were sonicated in air for 1 h, after which the mechanical properties and adhesion were measured as detailed below. No significant changes were observed (Figure S3 of the Supporting Information).

*Solid-State NMR Experiments.* SS-NMR experiments were conducted on a Bruker Avance 300 MHz SS-NMR instrument equipped with a 4 mm double-resonance VT cross-polarization magic-angle spinning (CPMAS) probe. The <sup>1</sup>H and <sup>13</sup>C carrier frequencies were 300.1 and 75.6 MHz, respectively. The magic-angle spinning (MAS) frequency was set to 12000 ± 3 Hz. The probe temperature was set to 297 K. The 90° pulses for <sup>1</sup>H and <sup>13</sup>C were 2.85–3.4 μs. The recycle delay and ramp cross-polarization (CP) times were 2 s and 1 ms, respectively. The receiver delay time was 6.5 μs, and the recycle delay time was 2 s for <sup>1</sup>H MAS single-pulse measurements. High-power two-pulse phase modulation decoupling with a field strength of 88 kHz was applied to the <sup>1</sup>H channel during an acquisition time of 55 ms. <sup>13</sup>C direct polarization (DP) MAS spectra were obtained with a recycle delay of 10 s in a pristine web under the dry condition at room temperature. This recycle time corresponded to 5 times the <sup>13</sup>C T<sub>1</sub> value of the carbonyl group, which showed the longest T<sub>1</sub> value in pristine webs. The <sup>13</sup>C chemical shift was referenced to the CH group of adamantane (29.46 ppm) as an external reference. <sup>1</sup>H MAS spectra were obtained by a simple single pulse with receiver delay of 6.5 μs and a recycle delay of 2 s. The <sup>1</sup>H chemical shift was referenced to tetrakis(trimethylsilyl)silane (0.2 ppm) as an external reference. <sup>1</sup>H–<sup>1</sup>H two-dimensional (2D) NOESY spectra were obtained by a conventional three-pulse method with a mixing time of 160 ms.<sup>22</sup> Time domain data in t<sub>1</sub> and t<sub>2</sub> were 512 and 2048 points, respectively. The maximal evolution time along t<sub>1</sub> was 2.56 ms. The total experimental time for 2D NOESY was ~2.5 h.

*Solution-State NMR Measurements.* Solution-state NMR <sup>1</sup>H Presat was conducted at 25 °C on an Agilent 750 MHz NMR instrument equipped with a cryo probe. The experiment was conducted in water spiked with 99.9% D<sub>2</sub>O as the lock solvent. A total of 512 scans were collected with a delay of 2 s and a pw90 pulse width of 6.5 μs.

**Removal of Salts for Adhesion Measurements.** Finally, we measured the adhesion of spider silk capture threads (pristine and washed) under the same conditions to determine how salts influence glycoprotein performance. To remove the salts, individual viscid threads from the webs spun by *L. cornutus* were mounted across 16 mm wide gaps in cardboard, immersed in deionized water, and then sonicated for 1 h. To control for the possibility that sonication per se influenced glycoprotein structure or function, measurements were also performed on viscid threads that were washed in deionized water without being sonicated. All threads were then stored in a P<sub>2</sub>O<sub>5</sub> desiccator. Finally, the threads were equilibrated at desired values of humidity at room temperature before adhesion was measured.

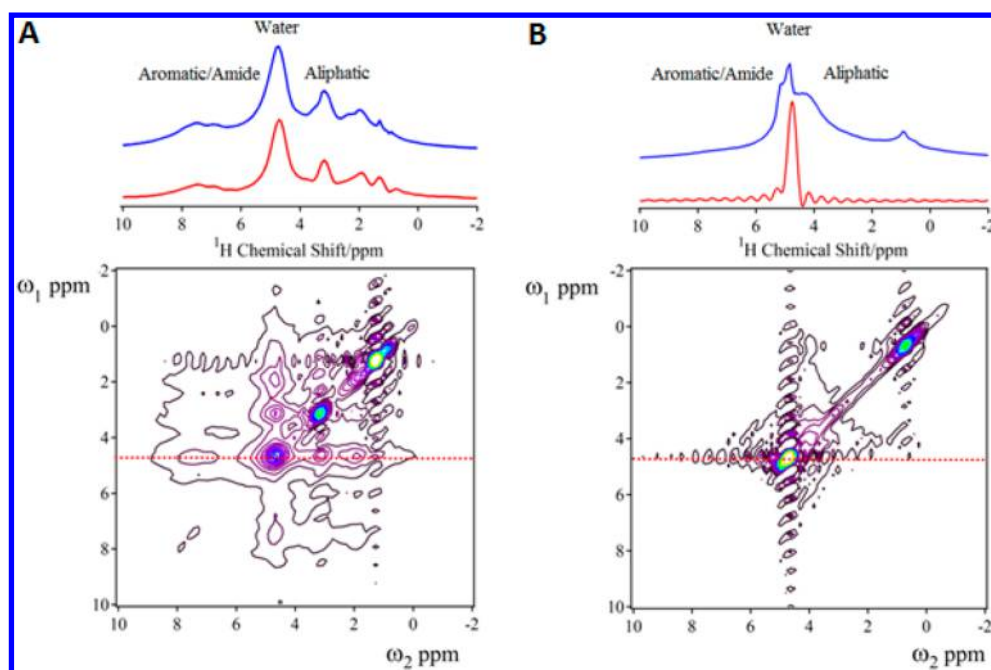


**Figure 1.** Effect of salt removal on the molecular mobility of spider silk. Shown are  $^1\text{H}$ – $^1\text{H}$  2D NOESY spectra of pristine (A) and washed (B) webs measured at high humidity (90% RH) and ambient temperature. The blue and red one-dimensional (1D) spectra are 1D  $^1\text{H}$  MAS and slice data of water molecules at 4.7 ppm (dotted line in 2D spectra), respectively. The general assignment of resonance peaks is mentioned. The water peak is at 4.7 ppm. The spinning rate used for these experiments was  $12000 \pm 3$  Hz. In pristine webs (A), all of the silk components interact with water, while that interaction is dramatically weakened when salts are removed (B).

**Adhesion Measurements.** To measure adhesion, viscid threads were suspended across 16 mm gaps in cardboard mounts at their innate tension. Experiments were performed using an MTS Nano Bionix instrument that measured force to  $\pm 1 \mu\text{N}$ . A clean glass plate with a width of 2 mm was fixed on a tack attached to the force sensor, while the cardboard mount with silk on it was fixed on the upper clamp. The silk was lowered at a rate of 0.1 mm/s until the thread made firm contact with the glass plate (force of  $10 \mu\text{N}$ ). After 60 s, the silk was pulled away from the glass plate at varied speeds (0.1, 1, and 2 mm/s), while the load–displacement behavior was recorded every 0.001 s. The force just before the silk thread released contact with the glass plate was recorded as the pull-off force, and these data were plotted as means  $\pm$  the standard deviation from 10 measurements. Pristine threads were taken from one orb web (so that there was no difference in the salt, protein, glycoprotein, or water composition of the threads from different webs). After the adhesion forces of pristine threads had been measured at different levels of humidity, the same threads were washed and sonicated to measure the adhesion forces in the absence of salts, thus making it a pairwise comparison. Comparisons were also made for an additional set of threads before and after sonication in a Branson 1510 instrument at 42 kHz for 1 h (in air) to verify that sonication itself did not influence the silk. No changes were detected (Figure S3 of the Supporting Information).

**Energy Model.** This model employed the principle of energy conservation and postulated that the work performed to pull a silk thread off a surface was consumed in both stretching of the axial silk and the energy required in peeling the glue droplets from the surface. The total work on the system ( $W_T$ ) is calculated by integrating the product of force  $f(h)$  times the infinitesimal height change  $dh$  from  $h$  to  $h + dh$ .

$$W_T = \int_{(h=0)}^{(h=h_T)} f(h) dh \quad (1)$$

The strain energy stored in the thread when it is pulled from its initial position until it separates from the surface,  $U_{\text{strain}}$ , is given by the following equation:

$$U_{\text{strain}} = \left[ \int_{(\varepsilon=0)}^{(\varepsilon=\varepsilon_T)} \sigma(\varepsilon) d\varepsilon \right] \pi r^2 (L - D) \quad (2)$$

where  $\sigma(\varepsilon)$  is the stress in a thread of radius  $r$  at a strain  $\varepsilon$ . Subtracting eq 2 from eq 1 gives the energy required to separate the glue droplets from the surface,  $U_{\text{glue}}$ . Representative tensile behavior curves are given in Figure S3A,B of the Supporting Information. The diameter of the threads was measured using scanning electron microscopy (JEOL) as shown in Figure S4 of the Supporting Information.

**Tensile Measurements.** To estimate the energy of adhesion using the energy model we previously developed,<sup>8</sup> tensile strain energy, stored in the capture threads before they release contact with the glass plate during adhesion measurements, needed to be determined. Capture threads, mounted across 16 mm cardboard gaps, were clamped on the Nano Bionix instrument such that the ends of the threads were fixed on upper and lower clamps. The tensile tests were performed at rates similar to what the thread experiences during adhesion measurements to account for any viscoelastic effects. The energy was computed as the area under the force–displacement curve.

**Optical Microscopy.** An Olympus BX51 camera was used to image threads. Panels A and B of Figure 4 show threads imaged at a 20 $\times$  magnification immediately after equilibration at 0 and 100% RH, respectively. The threads were mounted across cardboard gaps and were thus suspended while being imaged. For Figure 4C, a washed thread, equilibrated at 0% RH and suspended across a cardboard gap, was imaged at a 20 $\times$  magnification. For Figure 4D, a washed thread was placed on a microscopic slide and a few drops of deionized water were used to completely immerse the washed thread, followed by imaging at a 20 $\times$  magnification.

**Scanning Electron Microscopy.** Conductive carbon tape was used to cover the aluminum stubs. Individual threads (pristine or washed) were adhered to the tape and imaged under the scanning electron microscope (JEOL JSM-7401F field emission scanning electron microscope) at various magnifications (Figure S4 of the Supporting Information).

**Re-introduction of Salts.** Finally, salts were re-introduced to washed silk threads to determine if salt removal had reversible effects. Three different techniques were used. In the first approach, aqueous

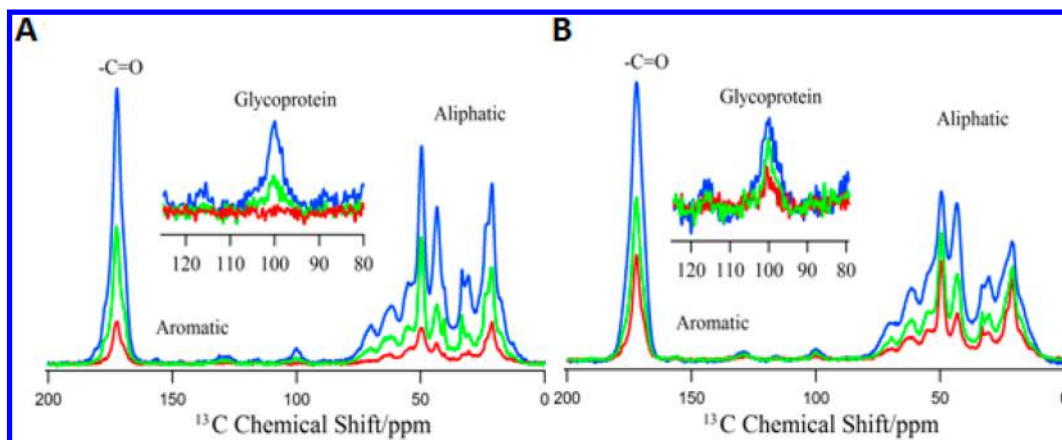


**Figure 2.** Influence of salt on glycoprotein mobility. Shown are  $^{13}\text{C}$  CPMAS NMR spectra of pristine (A) and washed (B) webs at ambient temperature and three different levels of humidity: 0% RH (blue), room (35% RH) humidity (green), and high (90% RH) humidity (red). The carbohydrate signal, representing the glycoproteins, is enlarged in the insets. The peak height increases with the rigidity of the molecules. Notice that significant reduction at lower RH occurs only when salts are present. The MAS frequency used was  $12000 \pm 3$  Hz.

solutions containing choline, glycine betaine, *N*-acetyltaurine, and/or isethionic acid (one to four of these compounds) at the correct concentrations<sup>9</sup> were prepared and put on a hydrophobic surface (contact angle of  $110^\circ$ ). Washed silk thread mounted on a cardboard piece was immersed in that solution for 3 h followed by sonication in the same solution for an additional 1 h. All salts were obtained from Sigma-Aldrich.

In the second approach, a water drop suspended from a pipet tip was moved along three pristine silk threads to collect their salts. The same water drop was placed on a hydrophobic surface, and washed capture threads mounted on a cardboard piece were immersed in it for 3 h followed by sonication in the same solution for an additional 1 h.

In the third approach, a pristine thread, equilibrated at 100% RH, was placed on a glass plate, very close to which a washed thread was placed, thus forming a composite thread. The composite threads were exposed to different values of humidity and were also sonicated for 1 h at room humidity ( $\sim 40\%$  RH).

## RESULTS

The salts observed (Figure S2 of the Supporting Information) were very similar to those found in previous studies, showing that the viscid silk spun by *L. cornutus* was similar in salt composition to the silks spun by species investigated in the past (*Nephila*, *Araneus*, and *Argiope*). Additionally, no proteins, carbohydrates, or glycoproteins were found in the aqueous extract, demonstrating that washing and sonication did not remove the proteins or glycoproteins from the viscid threads.<sup>9,24–27</sup>

First, we used solid-state  $^1\text{H}$  NMR to test how salts influenced molecular mobility. The  $^1\text{H}$  NMR in conjugation with magic-angle spinning (MAS) highlights mobile components in complex systems because high mobility weakens the dipolar coupling strength and leads to well-resolved  $^1\text{H}$  signals.<sup>28</sup> Because we used whole webs in this study, the signals have components from major ampullate proteins of dragline silk and flagelliform proteins of capture silk, in addition to salts and glycoproteins from the glue droplets. The  $^1\text{H}$  MAS spectrum of pristine webs at high humidity shows sharp, well-resolved signals that correspond to the highly mobile web components, while the spectrum of washed webs at high humidity shows broad signals (Figure 1, blue curves). This demonstrates that a large fraction of the silk in webs requires the presence of salts to become highly mobile on the NMR time scale.

Second, we determined the molecular proximity of water with the different web components (salts, fibrous proteins, and adhesive glycoproteins) using  $^1\text{H}$ – $^1\text{H}$  2D NOESY (proton–proton two-dimensional nuclear Overhauser effect spectroscopy) conjugated with MAS. This technique measures cross relaxations of protons that are close in space ( $<5$  Å), such that the initial buildup curve of the NOE intensity is, in a first approximation, proportional to  $1/r^6$  and  $\tau_c$ , where  $r$  is the distance between the two interacting protons and  $\tau_c$  is the correlation time for reorientation of the vector connecting two protons.<sup>29</sup> The 1D spectrum colored red in Figure 1A shows the  $^1\text{H}$  slice data of the water resonance at 4.7 ppm. In pristine webs, the overall line shapes of the slice data (red) are very consistent with the 1D  $^1\text{H}$  MAS spectrum (blue). In the case of washed webs (Figure 1B), the water peak in the slice data (red) is much sharper than that in the 1D  $^1\text{H}$  MAS data (blue), and the shapes of both curves are not consistent with each other. This suggests that all the components detected in the high-resolution 1D  $^1\text{H}$  MAS spectrum interact homogeneously and intimately with water only in the presence of salts (i.e., in pristine webs) and not when the salts are removed via washing.

$^1\text{H}$  MAS–NMR techniques show that salts are necessary for water to interact intimately with the web components and impart high mobility, but the glycoprotein signals overlap with the salt and protein signals<sup>30</sup> (in  $^1\text{H}$  NMR). Therefore, we also employed  $^{13}\text{C}$  NMR techniques to isolate the salt, protein, and glycoprotein signals. The  $^{13}\text{C}$  cross-polarization in conjugation with magic-angle spinning ( $^{13}\text{C}$  CP/MAS) relies on the  $^1\text{H}$ – $^{13}\text{C}$  dipolar coupling strength and therefore probes rigid molecules<sup>31</sup> (dynamic frequency of  $\leq 10^5$  Hz) such that the higher magnitude of the peaks signifies a higher rigidity, and vice versa. The  $^{13}\text{C}$  CP/MAS spectra for pristine silk and washed silk as a function of humidity are shown in Figure 2. The major ampullate and flagelliform proteins, as well as salts, manifest at 0–65 and  $>150$  ppm. In the washed web spectra, these regions show only the major ampullate and flagelliform proteins, because salts are absent. The  $^{13}\text{C}$  direct polarization magic-angle spinning (DP/MAS) spectra (Figure S5 of the Supporting Information) of pristine webs show narrow and tall peaks in these regions, indicating the high mobility of salts and silk protein components. In pristine webs, the CP/MAS peak magnitudes in these regions are reduced with an increase in humidity because of the increased mobility of the salts and

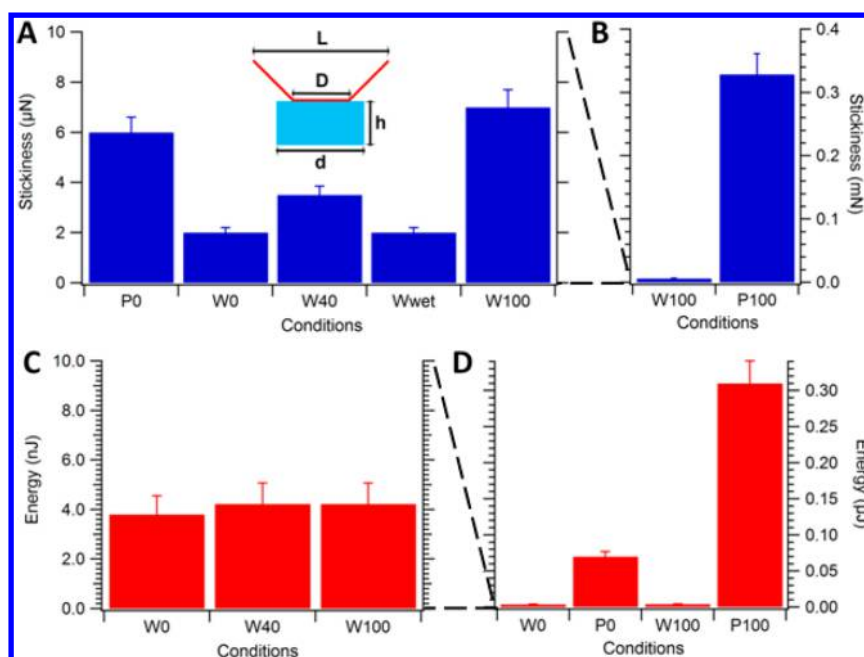


**Figure 3.** Effect of salts on the pull-off force and adhesion energy of capture threads. Panels A and B show the pull-off forces for pristine and washed capture threads, respectively, under different conditions. Notice the  $\sim 40$ -fold greater units for panel B. P and W indicate pristine and washed capture threads, respectively. The inset in panel A shows the setup used to measure the force of adhesion of single capture threads (red line) with a 2 mm wide clean glass plate (blue box). The inset defines the length variables when a single capture thread is separated from a clean glass surface. The difference in the stickiness units between panels A and B is emphasized using dotted lines. (C) Energy of adhesion of the glue drops of W threads under different conditions, calculated using the energy model developed previously by us.<sup>8</sup> (D) Energy of adhesion of P and W threads under different conditions. The difference in the energy units between panels C and D is emphasized using the dotted lines.

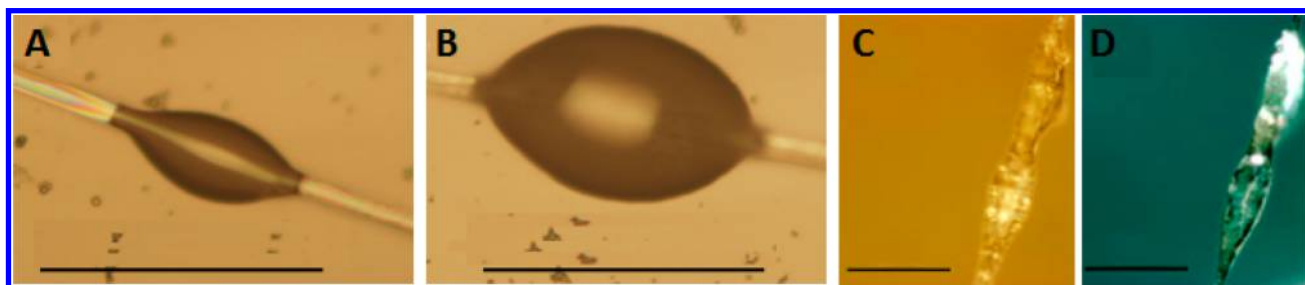


**Figure 4.** Effect of salts on the humidity response of the glue drops. (A and B) Optical images (Olympus BX51 camera) of single pristine glue drops at 0 and 100% RH, respectively. (C and D) Single glue drops of washed capture threads in air (equilibrated at 0% RH) and under water, i.e.,  $W_0$  and  $W_{wet}$ , respectively. Images were captured at a magnification of 20 $\times$ . Viscid silk in panels A–C was mounted across cardboard gaps while being exposed to the desired levels of humidity, while the thread in panel D was placed on a microscopic slide and completely immersed in deionized water. Pristine glue drops swell upon being exposed to humidity, while washed glue drops remain unaffected even when submerged in water. The scale bar for every image is 50  $\mu\text{m}$ . All measurements were performed at  $\sim 25$   $^{\circ}\text{C}$ .

protein domains that can accommodate water. In washed webs, the reduction in the size of the CP/MAS peak with an increase in humidity is due to the increased mobility of the protein domains only (salts are washed away). In addition to plasticizing major and minor ampullate silks, water can also plasticize the flagelliform proteins in the presence and, more interestingly, in the absence of salts. Plasticization of flagelliform proteins plays a major role in enhancing macro-scale adhesion of viscid threads (Figure 3). The reduction of the magnitude of CP/MAS signals also occurs in major ampullate proteins alone, during supercontraction of dragline silk.<sup>32</sup>

The main peak of interest, however, is the carbohydrate peak between 90 and 110 ppm. This peak arises exclusively from the glycoproteins<sup>23</sup> responsible for adhesion, and these glycoproteins are present only in the glue droplets. The insets in Figure 2 show the response of this peak to changes in humidity for

both pristine and washed webs. Because  $^{13}\text{C}$  CP/MAS NMR probes only rigid components, the glycoprotein peak becomes progressively weaker for pristine samples with increasing humidity such that at high humidity, the peak is indiscernible. This confirms the hypothesis that the glycoproteins are solvated by water. Upon comparison of the results for the pristine and washed webs, the changes in the glycoprotein signals are much weaker in washed webs as the humidity increases. This implies that the salts play a critical role in solvating the glycoproteins. The role of salts here goes beyond simply sequestering water because adding external water to the washed webs does not solvate the glycoproteins (insets in Figure 2). This is consistent with the physical appearance of the glycoproteins observed via optical and electron microscopy (Figure 4 and Figure S4A of the Supporting Information), where, in the presence of salts, the glycoprotein drops swell and, upon removal of salts, the

drops assume irregular shapes that are not affected by water. To rule out the possibility that sonication is denaturing the glycoproteins, these measurements were also performed on viscid silk threads that were washed in deionized water without sonication, and very similar results were obtained, implying that sonication is not denaturing the glycoproteins (Figure S6 of the Supporting Information).

The critical role of salts in solvating the glycoproteins manifests dramatically in “real-life” macro-scale adhesion of viscid threads when orb webs capture prey. To experimentally quantify whole thread adhesion, viscid threads mounted across cardboard gaps are brought in contact with a 2 mm wide clean glass surface and then retracted from the surface at controlled rates while the force–displacement response is recorded. Pristine viscid thread adheres 2 orders of magnitude more than washed thread (Figure 3A,B).<sup>33</sup> Moreover, the droplets on the washed thread collapse into hard solid blocks that do not establish a proper contact area and do not adhere to surfaces. Washed threads fail to adhere even after they have been slid on the glass substrate to preload them (Movie S1 of the Supporting Information), a routine technique for synthetic and natural adhesives, like the gecko’s toe,<sup>2</sup> that improves their contact with surfaces.

The solvation of glycoproteins by salts facilitates stronger adhesion at all levels of humidity. Figure 3A shows that a desiccated pristine thread ( $P_0$ ) adheres 3 times more strongly than a desiccated washed thread ( $W_0$ ). Also, a pristine thread equilibrated at 100% RH ( $P_{100}$ ) adheres 2 orders of magnitude more strongly than a washed thread equilibrated at 100% RH ( $W_{100}$ ) or a washed thread in which water is externally introduced ( $W_{\text{wet}}$ ). The small difference between the adhesion of  $W_{100}$  and  $W_{\text{wet}}$  is due simply to excess water disrupting van der Waals and hydrogen bonding between  $W_{\text{wet}}$  and the substrate. While this demonstrates that salts alone induce adhesion, the salts clearly act synergistically with water, as shown by a dramatic two-order of magnitude difference in the adhesion between the pristine and washed threads at 100% RH [ $P_{100}/W_{100} > 10^2$  in the presence of water (Figure 3B)] compared to the more modest 3-fold difference at 0% RH ( $P_0/W_0 \sim 3$  in the absence of water). Water alone does not facilitate adhesion because  $W_{\text{wet}} < W_{100} \ll P_{100}$ , whereas salts alone are capable of promoting adhesion, although not as strongly as in the presence of water ( $P_{100}/P_0 \sim 10^2/3$ ).

An energy model, developed previously by us,<sup>8</sup> is used to determine whether the differences in force values are due to changes in the adhesion of glue drops ( $U_{\text{glue}}$ ) under different conditions or to variation in the tensile properties of the axial silk fibers ( $U_{\text{strain}}$ ), because flagelliform proteins are plasticized by water even in the absence of salts. The values of  $U_{\text{glue}}$  depend on intermolecular adhesion, as well as on the energy required to stretch the glue droplets (details given in the Experimental Section). Using this energy model, the  $U_{\text{glue}}$  values for  $W_0$  and  $W_{100}$  are equal (Figure 3B), implying that the difference in their total adhesion force is due primarily to the axial silk fibers becoming softer and more extensible, even in the absence of salts, with increasing humidity. According to our model, softening of the threads occurs rather than a change in the adhesion of individual glue droplets. This observation is supported by optically imaging  $W$  threads in air at 0% RH, at 100% RH, and under water, which show no differences in the sizes of glue drops (glycoprotein blocks) (Figure 4C,D). It also indicates that the glycoprotein, after washing, does not interact with water because water does not infiltrate its collapsed

structure. In comparison, the glue drops of the pristine thread expand with increases in humidity (Figure 4A,B), as previously observed.<sup>34</sup> The irregular shape of the drops after washing contrasts with their regular (ellipsoidal) shape prior to washing and indicates that the glycoproteins collapse and harden only after salts are removed.

Further investigation using the energy model confirms that the two order of magnitude difference in adhesion force between  $P_{100}$  and  $W_{100}$  is due to the difference in the adhesion of their glue drops rather than changes in their axial silk’s tensile characteristics because the  $U_{\text{glue}}$  values are two orders of magnitude higher for the pristine thread ( $0.31 \mu\text{J}$ ) than for the washed thread ( $0.004 \mu\text{J}$ ) (Figure 3C,D). Also, the significant difference in the  $U_{\text{glue}}$  values of  $P_0$  and  $W_0$  (Figure 3D) emphasizes the stronger adhesion exhibited by pristine glue droplets compared to washed glue droplets, even in the absence of water. These macro-scale adhesion results, combined with optical imaging, clearly show that the difference in the adhering capabilities of the pristine and washed threads is due to the salts solvating the glycoproteins and are thus in close agreement with the molecular evidence provided by SS-NMR.

## DISCUSSION

To capture prey and act like an effective adhesive, the glycoproteins in spider silk aggregate glue have to be mobile and make good contact with the substrate, such as an insect’s exoskeleton. SS-NMR results, combined with adhesion measurements and optical observations, provide a molecular and macro-scale picture of the role of salts in solvating the glycoproteins and allowing their mobility. The  $^{13}\text{C}$  CP/MAS results are extremely sensitive to mobility. For example, solidlike samples will show the strongest peak, and the magnitude of this peak will decrease dramatically with even small increases in mobility. For this reason, the consistent reduction in the glycoprotein peaks for the pristine sample as humidity increases and the much weaker changes in the glycoprotein peaks for the washed sample (Figure 2) are direct proof of the role of salts in helping to solvate the glycoproteins. On the other hand,  $^1\text{H}$ – $^1\text{H}$  NOESY results (Figure 1) are extremely sensitive to the proximity of water protons in other molecules. Even though some water may be absorbed by the glycoproteins when salts are absent, as shown by the weak reduction in the glycoprotein peak intensity in washed webs (Figure 2B), it is insufficient to completely mobilize the glycoproteins, which is indicated by the indiscernible cross-peaks in the washed webs.

On the basis of our experimental results and observations, we show that salts are present in the bulk of the glycoprotein glue itself, rather than just as a “coating”, as previously hypothesized.<sup>11</sup> This allows the salts to solvate the bulk of the glycoproteins, thus allowing and enhancing adhesion, even under dry conditions. The hygroscopic nature of the salts<sup>9</sup> combined with their presence in the bulk of the glycoproteins facilitates intimate interaction of the latter with water molecules (Figures 1 and 2), which helps in swelling the glue drops at high levels of humidity (Figure 4).

On the basis of our results, we hypothesize that salts solvate the glycoproteins by “screening” the interactions between the glycoprotein molecules, thus increasing their solubility. This phenomenon is termed “salting in” and is observed in some natural<sup>35</sup> and synthetic systems.<sup>36</sup> Pristine glue acts like a viscoelastic solid, which indicates the presence of cross-linking.<sup>8</sup> This cross-linking and the phase separation of the glycoproteins

from the aqueous shell obviously take place after the spider has coated the flagelliform silk fibers with the aqueous glue-salt dope from its aggregate glands. We suggest that salts allow glycoproteins to stay in solution inside the aggregate glands so that the glycoproteins can be coated onto flagelliform silk when viscid threads are spun. Upon removal of salts from viscid threads, the cross-linked glycoproteins collapse because of intra- and intermolecular interactions, now possible because of the absence of the screening effect of the salts, and form a hard solid block. Surprisingly, unlike typical natural and synthetic systems that require salting in, re-introduction of water and salts into a washed silk thread does not resolvent and reswell the glue droplets (Figure S7 of the Supporting Information). We suggest that interactions between the functional groups on the glycoprotein molecules, in the absence of the charge-screening effect of salts, result in excessive bond formation, which precludes resolution and reswelling of glycoproteins. Such a phenomenon has been observed in silica aerogels.<sup>37</sup> Loss of adhesion upon removal of salts is thus irreversible on the time scale of our measurements. Additional experimentation is required to understand the actual mechanism of the solvation of glycoproteins by salts.

The irreversible response of the glue droplets upon re-addition of salts (Figure S7 of the Supporting Information) is intriguing considering that the spider webs often experience heavy rain, and this should affect the ability of spiders to capture prey if the salt is washed away from the glue droplets. Although systematic studies measuring adhesion before and after rain are lacking, some qualitative studies suggest that the capture silk is less sticky after the rains. However, such considerations are largely trivial because most orb web spiders remove their webs during rains.<sup>38</sup> This behavior is likely in response to the physical damage caused by rain droplets to the viscid threads but also allows spiders to recover the salts, by eating the remaining web, before they are washed away. It is particularly noteworthy that silk recycling does not occur in most web-spinning spiders and is largely confined to orb web spiders that produce viscid silk threads.<sup>39</sup>

## CONCLUSION

Viscid threads evolved at least 150 million years ago in araneoid spiders and are now used by more than 95% of the world's ~4500 species of orb spiders.<sup>6</sup> The ancestor of these spiders coated capture threads in its orb web with a sheath of dry adhesive cribellate nanofibers (primitive cribellar threads) that adhere primarily through van der Waals forces.<sup>40</sup> Cribellate threads lose adhesion when wetted because of clumping of the nanofibers,<sup>41</sup> while the viscid threads of araneoid spiders function poorly when dry.<sup>19</sup> Thus, while phylogenetic evidence strongly demonstrates the homology of these two types of orb webs,<sup>1,26</sup> there is no clear hypothesis for how spiders underwent the transition from one type of adhesive silk to the other. It is suggested that evolution of viscid threads entails the gradual cessation of cribellate thread production combined with the increasingly important role played by the viscous material (salts and glycoproteins) in viscid thread adhesion.<sup>43</sup> Our data describe the latter and thus suggest a plausible hypothesis for how this evolutionary transition in bioadhesives might have occurred. Initially, salts were incorporated into cribellate threads<sup>41</sup> because salts facilitate adhesion even in dry silk. Cribellate silk represents the earliest known spider adhesive, and while the van der Waals-based adhesion of primitive cribellate nanofibers is independent of humidity,<sup>40</sup> the

nanofibers of derived cribellate threads have a noded morphology that makes them responsive to humidity because their nanostructure allows for additional hygroscopic adhesion.<sup>40</sup> The hygroscopic nature of the salts would facilitate this added adhesion, and we speculate that even slight increases in the presence of salts set up a tipping point that favors the origin of the large viscoelastic glue droplets and glycoproteins of viscid silk, an adhesive that is superior in both stickiness and material economy to ancestral cribellate adhesives.<sup>42</sup>

## ASSOCIATED CONTENT

### Supporting Information

A movie showing the sliding of washed viscid silk, a figure showing solution-state <sup>1</sup>H NMR of the aqueous extract of webs and its interpretation, a figure showing tensile and adhesive behavior of threads before and after sonication, a figure showing electron micrographs of pristine and viscid threads, a figure showing <sup>13</sup>C DP/MAS spectra of pristine silk threads, a figure showing <sup>13</sup>C CP/MAS spectra of pristine threads and threads washed without sonication, the results of re-introduction of salts, and a related figure. This material is available free of charge via the Internet at <http://pubs.acs.org>.

## AUTHOR INFORMATION

### Corresponding Author

\*E-mail: [ali4@uakron.edu](mailto:ali4@uakron.edu).

### Notes

The authors declare no competing financial interest.

## ACKNOWLEDGMENTS

We sincerely thank Venkat Dudipala, Liladhar Paudel, and Stephanie M. Bilinovich for their assistance with <sup>1</sup>H solution-state NMR. Chelsea A. Goliass helped with the optical imaging of panels A and B of Figure 4. This work was supported by the National Science Foundation [Grants DMR-0512156 (A.D.), DMR-1105370 (A.D.), and IOS-1257809 (T.A.B. and A.D.)] and the NSF-REU program (A.D.). We also acknowledge funding from the Austen Bioinnovation Institute in Akron (ABIA), I-Min Tso from Tunghai University, and The University of Akron's Integrated Bioscience and Tiered-mentoring programs.

## REFERENCES

- (1) Lin, Q.; Gourdon, D.; Sun, C.; Holten-Andersen, N.; Anderson, T. H.; Waite, J. H.; Israelachvili, J. N. *Proc. Natl. Acad. Sci. U.S.A.* **2007**, *104*, 3782–3786.
- (2) Autumn, K.; Liang, Y. a.; Hsieh, S. T.; Zesch, W.; Chan, W. P.; Kenny, T. W.; Fearing, R.; Full, R. J. *Nature* **2000**, *405*, 681–685.
- (3) Autumn, K.; Sitti, M.; Liang, Y. a.; Peattie, A. M.; Hansen, W. R.; Sponberg, S.; Kenny, T. W.; Fearing, R.; Israelachvili, J. N.; Full, R. J. *Proc. Natl. Acad. Sci. U.S.A.* **2002**, *99*, 12252–12256.
- (4) Hanna, B. Y. G.; Barnes, W. J. O. N. P. *J. Exp. Biol.* **1991**, *155*, 103–125.
- (5) Dickinson, G. H.; Vega, I. E.; Wahl, K. J.; Orihuela, B.; Beyley, V.; Rodriguez, E. N.; Everett, R. K.; Bonaventura, J.; Rittschof, D. *J. Exp. Biol.* **2009**, *212*, 3499–3510.
- (6) Blackledge, T. A.; Scharff, N.; Coddington, J. A.; Szüts, T.; Wenzel, J. W.; Hayashi, C. Y.; Agnarsson, I. *Proc. Natl. Acad. Sci. U.S.A.* **2009**, *106*, 5229–5234.
- (7) Denny, M. *J. Exp. Biol.* **1976**, *65*, 483–506.
- (8) Sahni, V.; Blackledge, T. A.; Dhinojwala, A. *Nat. Commun.* **2010**, *1*, 19.

- (9) Vollrath, F.; Fairbrother, W. J.; Williams, R. J. P.; Tillinghast, E. K.; Bernstein, D. T.; Gallagher, K. S.; Townley, M. A. *Nature* **1990**, *345*, 526–528.
- (10) Tillinghast, E. K. *Naturwissenschaften* **1981**, *68*, 3–4.
- (11) Vollrath, F.; Tillinghast, E. K. *Naturwissenschaften* **1991**, *78*, 557–559.
- (12) Opell, B. D.; Hendricks, M. L. *J. Exp. Biol.* **2010**, *213*, 339–346.
- (13) Ohgo, K.; Kawase, T.; Ashida, J.; Asakura, T. *Biomacromolecules* **2006**, *7*, 1210–1214.
- (14) Lee, K. S.; Kim, B. Y.; Je, Y. H.; Woo, S. D.; Sohn, H. D.; Jin, B. R. *J. Biosci.* **2007**, *32*, 705–712.
- (15) Hayashi, C.; Lewis, R. V. *J. Mol. Biol.* **1998**, *275*, 773–784.
- (16) Hayashi, C. Y.; Shipley, N.; Lewis, R. V. *Int. J. Biol. Macromol.* **1999**, *24*, 271–275.
- (17) Chores, O.; Bayarmagnai, B.; Lewis, R. V. *Biomacromolecules* **2009**, *10*, 2852–2856.
- (18) Dreesbach, K.; Uhlenbruck, G.; Tillinghast, E. K. *Insect Biochem.* **1983**, *13*, 627–631.
- (19) Vollrath, F.; Edmonds, D. T. *Nature* **1989**, *340*, 305–307.
- (20) Blackledge, T. A.; Hayashi, C. Y. *J. Exp. Biol.* **2006**, *209*, 3131–3140.
- (21) Higgins, L. E.; Townley, M. A.; Tillinghast, E. K.; Rankin, M. A. *J. Arachnol.* **2001**, *29*, 82–94.
- (22) Wüthrich, K.; Wider, G.; Wagner, G.; Braun, W. *J. Mol. Biol.* **1982**, *155*, 311–319.
- (23) Bonthrone, K. M.; Vollrath, F.; Hunter, B. K.; Sanders, J. K. M. *Proc. R. Soc. B* **1992**, *248*, 141–144.
- (24) Townley, M. A.; Pu, Q.; Zercher, C. K.; Neefus, C. D.; Tillinghast, E. K. *Chem. Biodiversity* **2012**, *9*, 2159–2174.
- (25) Townley, M. A.; Bernstein, D. T.; Gallagher, K. S.; Tillinghast, E. K. *J. Exp. Zool.* **1991**, *259*, 154–165.
- (26) Townley, M. A.; Tillinghast, E. K.; Neefus, C. D. *J. Exp. Biol.* **2006**, *209*, 1463–1486.
- (27) Anderson, C. M.; Tillinghast, E. K. *Physiol. Entomol.* **1980**, *5*, 101–106.
- (28) Evdokimov, A. M.; Moskalev, V. V.; Talanov, V. L.; Kolonistov, V. P.; Andreev, A. S.; Perepelkin, K. E. *Mech. Compos. Mater.* **1982**, *17*, 642–646.
- (29) Otting, G.; Wüthrich, K. *Q. Rev. Biophys.* **1990**, *23*, 39–96.
- (30) Byrne, C. M. P.; Hayes, M. H. B.; Kumar, R.; Novotny, E. H.; Lanigan, G.; Richards, K. G.; Fay, D.; Simpson, A. J. *Water Res.* **2010**, *44*, 4379–4390.
- (31) Taylor, R. E. *Concepts Magn. Reson., Part A* **2004**, *22*, 37–49.
- (32) Holland, G. P.; Jenkins, J. E.; Creager, M. S.; Lewis, R. V.; Yarger, J. L. *Biomacromolecules* **2008**, *9*, 651–657.
- (33) There can be some differences in the adhesion of capture threads depending on diet, environment, population, etc., as shown in: Higgins, L. E.; et al. *J. Arachnol.* **2001**, *29*, 82–94. However, the adhesion value results shown in our study are based on pairwise comparisons.
- (34) Sahni, V.; Blackledge, T. A.; Dhinojwala, A. *Sci. Rep.* **2011**, *1*, 41.
- (35) Arakawa, T.; Timasheff, S. N. *Biochemistry* **1984**, *23*, 5912–5923.
- (36) Swann, J. M. G.; Bras, W.; Topham, P. D.; Howse, J. R.; Ryan, A. J. *Langmuir* **2010**, *26*, 10191–10197.
- (37) Venkateswara Rao, A.; Nilsen, E.; Einarsrud, M.-A. *J. Non-Cryst. Solids* **2001**, *296*, 165–171.
- (38) Opell, B. D. *Funct. Ecol.* **1998**, *12*, 613–624.
- (39) Lubin, Y. D. In *Spiders: Webs, Behavior, and Evolution*; Shear, W. A., Ed.; Stanford University Press: Stanford, CA, 1986; pp 132–171.
- (40) Hawthorn, A. C.; Opell, B. D. *J. Exp. Biol.* **2003**, *206*, 3905–3911.
- (41) Liao, X.; Yin, G.; Huang, Z.; Yao, Y.; Gu, J.; Han, D. *Mater. Sci. Eng., C* **2011**, *31*, 128–133.
- (42) Griswold, C. E.; Coddington, J. A.; Platnick, N. I.; Forster, R. R. *J. Arachnol.* **1999**, *27*, 53–63.
- (43) Opell, B. D.; Tran, A. M.; Karinshak, S. E. *J. Exp. Zool., Part A* **2011**, *315A*, 376–384.